Agricultural and Forest Meteorology 345 (2024) 109827

Contents lists available at ScienceDirect

Agricultural and Forest Meteorology

journal homepage: www.elsevier.com/locate/agrformet

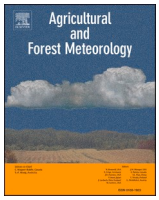

Soil water components control plant water uptake along a subalpine elevation gradient on the Eastern Qinghai-Tibet Plateau

Juying Sun [a,b], Xiangyang Sun [a,*], Genxu Wang [a,b,*], Wenchang Dong [c], Zhaoyong Hu [a], Shouqin Sun [a], Fei Wang [b], Chunlin Song [a], Shan Lin [a]

[a] State Key Laboratory of Hydraulics and Mountain River Engineering, College of Water Resource and Hydropower, Sichuan University, Chengdu 610065, China
[b] Institute of Mountain Hazards and Environment, Chinese Academy of Sciences, Chengdu 610041, China
[c] Zhejiang Design Institute of Water Conservancy & Hydro-Electric Power Co., Ltd., Hangzhou 310002, China

ARTICLE INFO

Keywords:
Stable water isotopes
Root water uptake
Soil moisture
Plant–available water
Elevational gradient

ABSTRACT

Soil water is crucial for maintaining forest health by providing plants with a dependable water source. However, the understanding of the impact of soil moisture on plant water uptake, particularly in conditions of excess soil water, is limited. In this study, we investigated root water uptake strategies of dominant species along an elevational gradient in the subalpine region of the eastern Qinghai–Tibet Plateau. Our results demonstrated divergent relationships between soil moisture and water uptake fractions in the shallow soil layer, where moisture generally exceeds field capacity (θ_{fc}) during the growing season, and in the deep soil layer, showing negative and positive associations, respectively. This disparity is linked to soil water components: when plants mainly used shallow soil water, the relative proportion of plant–available water (the part of water between wilting coefficient and θ_{fc}) in the shallow soil was smaller compared to instances where plants mainly used deep soil water. Conversely, the pattern for gravity water was the opposite. This phenomenon is attributed to precipitation replenishing shallow soil with gravity water and deep soil with plant–available water, leading to poor aeration in the shallow soil and an abundance of plant–available water in the deep soil, and plants tended to shift to deep soil water as a result. Furthermore, the decrease in the relative proportion of plant–available water in the shallow soil along the elevational gradient results in plants in the lowest-altitude broadleaf forest obtaining more shallow soil water and less deep soil water, which can also enhance our understanding of how soil moisture components influence plant water–use strategies. Additionally, no hydrological niche segregation was observed among species in this humid environment. These results can improve our comprehension of soil–plant interactions in subalpine areas.

1. Introduction

Plant transpiration is the primary consumption in terrestrial ecosystems, and plays a pivotal role in the global hydrological cycle (Good et al., 2015; Lian et al., 2018). The status of plant water uptake regulates plant growth and ecosystem productivity (Xu et al., 2011). A thorough understanding of plant water sources not only enhances our grasp of hydrological processes at the soil–plant interface, thus refining hydrological modelling (Jing et al., 2014; Yang et al., 2022; Zheng and Wang, 2007), but also provides insights into plant survival strategies and their adaptive responses to climate change (Cheng et al., 2006; Xu et al., 2011; Zhu and Jia, 2011).

The strategies for root water uptake (RWU) in plants are influenced by species, morphology and environmental conditions (Ellsworth and Sternberg, 2015; Li et al., 2002; Thomas et al., 2020). The soil serves as a vital water source for plant survival, with its availability being a pivotal factor influencing the variability in plant water uptake patterns (Zhou et al., 2019). One the one hand, plants trend to change water use strategies to deal with water scarcity, such as a deeper water source as soil moisture (SM) decreases (Brinkmann et al., 2019; Köcher et al., 2012) or exhibiting hydrological niche segmentation to avoid water competition in coexisting species (Muñoz-Villers et al., 2020; Silvertown et al., 2015). Consequently, augmented soil water content, generally the part below field capacity, can stimulate plant growth. On the other hand, excessive soil moisture can hinder plant growth. When soil water exceeds field capacity, the increased gravity water in the large pores may

* Corresponding authors.
E-mail addresses: sunxy@scu.edu.cn (X. Sun), wanggx@scu.edu.cn (G. Wang).

https://doi.org/10.1016/j.agrformet.2023.109827
Received 9 October 2022; Received in revised form 17 November 2023; Accepted 24 November 2023
Available online 12 December 2023
0168-1923/© 2023 Elsevier B.V. All rights reserved.

induce anoxic conditions and reduced aeration (Dash et al., 2022), subsequently influencing soil bacterial diversity, as well as root morphology and activity (Li et al., 2020; Sajedi et al., 2012). Therefore, changes in soil water components may significantly impact RWU (Peters et al., 2017; Yang and Jong, 1971; Zhang et al., 2020). However, there is a lack of comprehensive understanding regarding how soil water components affect patterns of RWU, potentially limiting our comprehension of the SM–RWU relationship.

Subalpine areas are highly susceptible to climate change(Panthi et al., 2020; Vitasse et al., 2021), and their elevation gradients provide different environmental gradients such as climate, biodiversity, and soil properties (Feng et al., 2021; Vetaas et al., 2019; Xu et al., 2018). This unique combination makes subalpine elevation gradients an excellent location for studying the response of hydrological processes to climate change (Goulden et al., 2012; Ma et al., 2019; Sun et al., 2020; Zhu et al., 2016). The elevational patterns of some hydrological processes, such as evaporative fluxes (Hu et al., 2018; Jung et al., 2014; van den Bergh et al., 2013), water use efficiency (Nandy et al., 2022; Wang et al., 2021; Wu et al., 2015) and snow water equivalent (Capelli et al., 2022; Della Chiesa et al., 2014; Musselman et al., 2017) have been well described in subalpine regions. However, the subalpine elevation pattern of RWU is poorly understood in mountainous areas, and only a few studies conducted RWU along elevational gradients, which focused on cloud water uptake, seasonal origins of plant water use (Berry et al., 2014; Juhlke et al., 2021; Rossatto et al., 2012). Limit information on the elevational patterns of water uptake patterns of plants weaken our understanding of ecohydrological processes and soil–plant interactions in subalpine areas.

Due to no fractionation occurs during RWU and stem vessel transport, except in some xerophytes or halophytes (Chen et al., 2020b; Dawson et al., 2002; Sprenger et al., 2016), the hydrogen and oxygen stable isotopes (δ^2H, $\delta^{18}O$) have widely used to determine water sources of plants in various ecosystems (Beyer et al., 2018; Liu et al., 2021, 2019; Penna et al., 2020). This method has been applied herein to investigate the water uptake patterns of dominant species along the elevational gradient of Mount Gongga. This study aims to (1) to assess the spatial and seasonal patterns of the water uptake strategies of plants along a subalpine elevation gradient and (2) to explore how soil water components influence water uptake patterns.

2. Materials and methods

2.1. Study sites and their microclimate condition

The study was conducted in the Hailuogou catchment on the eastern edge of Mount Gongga on the eastern edge of the Qinghai–Tibet Plateau with the elevation ranging from 1414 m a.s.l to 7443 m a.s.l. Three sampling sites are located in the forest region of the Hailuogou catchment (Fig. 1). The broadleaf forest (BF) site is situated at 29.596°E, 102.048°N, at an elevation of 2200 m a.s.l. The dominant species of BF include *Lithocarpus cleistocarpus* and *Decaisnea fargesii Franch*. The broadleaf and coniferous mixed forest (MF) site is located at 29.586°E, 102.026°N, with an elevation of 2810 m a.s.l. The dominant species of MF are *Abies fabri, Picea brachytyla, Acer campbellii.* and *Rhododendron simsii Planch*. The coniferous forest (CF) site is located at 29.571°E, 101.985°N, with an elevation of 3100 m a.s.l. The dominant species include *Abies fabri, Sorbus pohuashanensis and Rhododendron simsii Planch.*

Precipitation and air temperature were recorded in the three sampling sites using auto meteorological observation systems, details can be found in Hu et al. (2018). Precipitation was not evenly distributed during 2018 to 2019, with a peak in June 2018 and July 2019 (Fig. 2a). Within the three sites, CF was the most humid, with annual precipitation of 2167 mm and 1805 mm in 2018 and 2019, respectively. BF had the lowest precipitation, with annual precipitation values of 1858 mm and 1365 mm, respectively. Additionally, the results showed that 2019 was drier, with less than approximately 400 mm of precipitation on average (approximately 20 %) than that in 2018. According to the weather station data from the 3000–m field research station of Mount Gongga (http://ggf.cern.ac.cn/), the temperature increased significantly at a rate of 0.04 °C from 1988 to 2019 ($p<0.01$, Fig. 2c), while the precipitation decreased significantly at a rate of 6.51 mm year^{-1} ($p<0.01$), showing the climate change characteristics of "warming and drying". Precipitation in 2019 was close to the linear fitting line, which was 12.8 % lower than the precipitation in 2018. Therefore, 2018 and 2019 were defined as a wet year and a normal year in this study, respectively.

2.2. Sample collection and isotopic analyses

From May to October in 2018 and 2019, plant samples and soil samples were collected once a month in three forest ecosystems along the elevational gradient. To represent the dominant vegetation of the

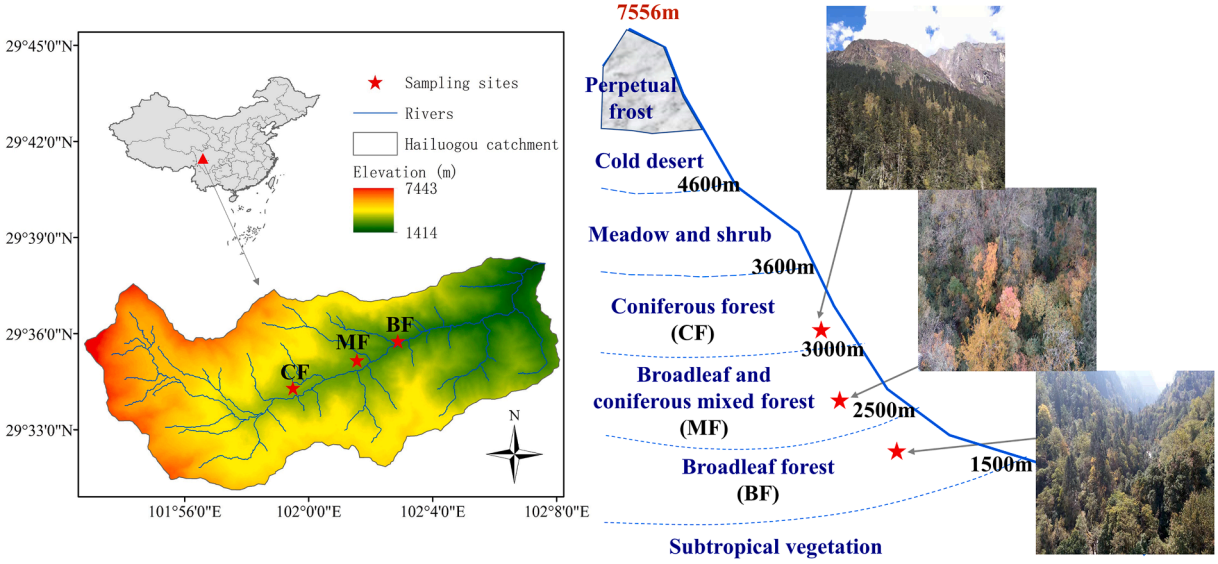

Fig. 1. Locations of the study area and the sampling sites.

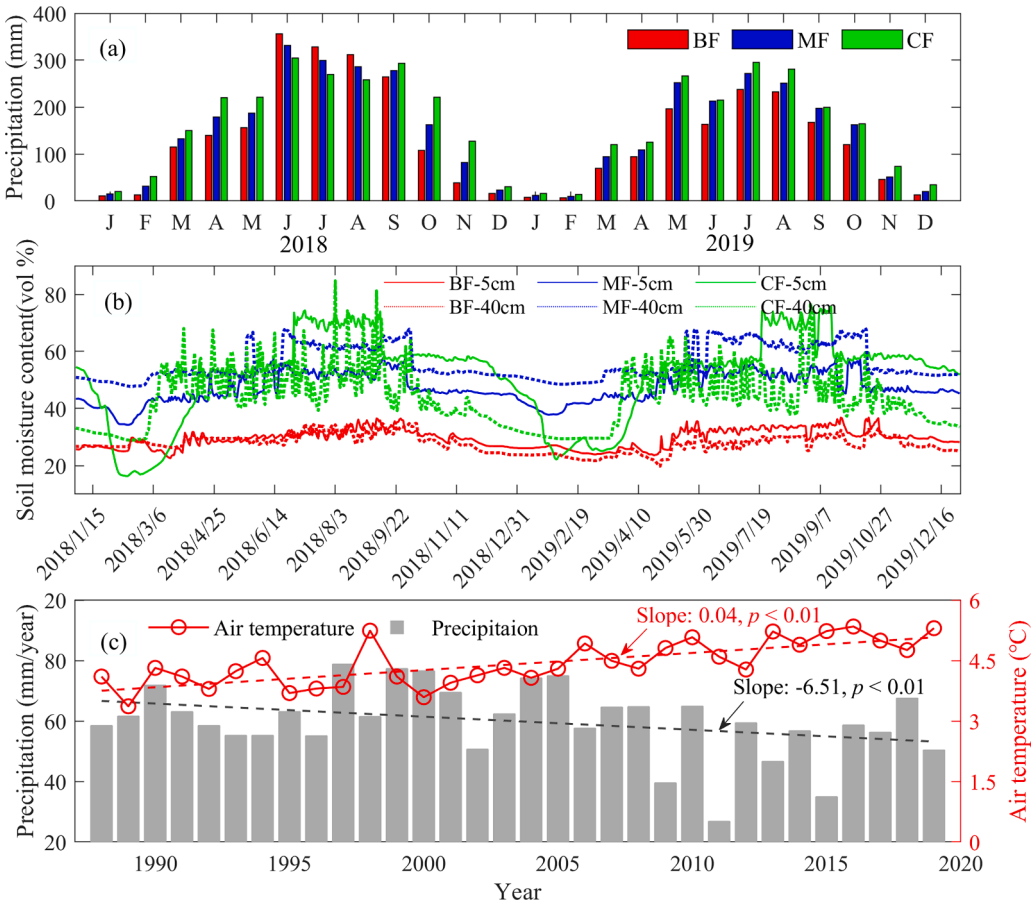

Fig. 2. Hydrometeorological conditions in 2018 and 2019 for (a) precipitation, (b) volumetric soil moisture at 5 cm and 40 cm, and (c) trends of annual precipitation and air temperature at 3000 m from 1988 to 2019 in Mount Gongga.

study area, we selected nine woody species (including dominant trees and shrubs), and the basic characteristics of the sampled species are described in Table 1. For each species, xylem samples were collected from 3 to 5 individual plants, and three replicates were collected from each plant. Outer bark and phloem tissue were removed from the xylem samples and then placed into 10–ml glass vials, peeled with parafilm, and kept frozen at −18 °C. Soil samples were collected at 10–cm intervals in the 0–100 cm range on each collection date around the sampling species, and three replicates of soil samples were collected for each soil depth. Soil samples were divided into two parts: one was placed in 10–cm glass vials, peeled with parafilm, and kept frozen at −18 °C for isotope analysis, and the other was employed to determine the gravimetric soil water content (GWC,%) by drying for 24 h at 105 °C. Besides, root biomass was gathered from 50 cm × 50 cm quadrats ($n = 3$) at the 0–40–cm soil and 40–100–cm soil.

The plant xylem water and bulk soil water were extracted by a cryogenic vacuum distillation system (LI–2100, LICA United Technology Limited, China). The gravimetric soil water content of xylem samples was derived by the relative mass change before and after the xylem water extraction by LI–2100. The stable isotope composition ($\delta^{18}O$ and $\delta^{2}H$) of water samples was analysed by isotope ratio infrared spectroscopy LGR (LWIA, Los Gatos Research, Canada) based on off–axis integrated cavity output spectroscopy at the Institute of Mountain Hazards and Environment, CAS. All water samples were analysed 6 times, and the average value of the final 4 times was used to remove the contamination of the last sample. The ratio of stable isotopes is expressed as follows:

$$\delta(‰) = \left(\frac{R_{sam}}{R_{std}} - 1\right) \times 1000 \quad (1)$$

where (‰) is the ratio of $^{2}H/^{1}H$ and $^{18}O/^{16}O$ relative to Vienna Standard Mean Ocean Water (V–SMOW), and R_{sam} and R_{std} are the ratio of heavy isotopes to light isotopes ($^{2}H/^{1}H$ and $^{18}O/^{16}O$) of samples and standards (V–SMOW), respectively. The measurement accuracies of $\delta^{2}H$ and $\delta^{18}O$

Table 1
Basic characteristics of the sampled tree species.

Sites	Elevation (m)	Temperature and precipitation	Tree species	*Code*	Tree/Shrub	Mean breast diameter (cm)	Mean height (m)
BF	2200	8.20 °C,	*Lithocarpus cleistocarpus*	*Lc*	Tree	31.5	17.9
		1612 mm	*Decaisnea fargesii Franch*	*Df*	Shrub	12.1	2.4
MF	2810	6.32 °C,	*Abies fabri*	*Af*	Tree	40.2	28.1
		1825 mm	*Picea brachytyla*	*Pb*	Tree	37.6	27.4
			Acer campbellii	*Ac*	Tree	19.7	8.5
			Rhododendron simsii Planch	*Rp*	Shrub	11.4	2.4
CF	3100	3.59 °C,	*Abies fabri*	*Af*	Tree	42.8	25.3
		1986 mm	*Sorbus pohuashanensis*	*Sp*	Shrub	8.4	2.4
			Rhododendron simsii Planch	*Rp*	Shrub	11.2	2.1

were ±1‰ and ±0.2‰, respectively. To eliminate the effect of organic contaminants (such as methanol and ethanol), all isotope values were examined using the Spectral Contamination Identifier post–processing software (Los Gatos Research, Inc.). Once spectral interference occurs, the isotope data were corrected using a standard curve created by engineers from Los Gatos Research (Schultz et al., 2011).

2.3. Water source partitioning

A Bayesian mixing model (Stable Isotope Mixing Models in R, R package 'simmr'), which aims to solve mixing equations for stable isotopic data within a Bayesian structure, was used to determine the proportional contributions of soil water at different soil depths (Parnell and Inger, 2016). Based on a mass balance equation of δ^2H and $\delta^{18}O$, this model used linear stable isotope mixing models. The model used the Markov chain Monte Carlo (MCMC) approach fitting to estimate parameters. The method enables the inclusion of uncertainty in the sources, water mixture (plant xylem water), and their residuals. The MCMC repeatedly makes educated guesses about the values of the water uptake proportion and finds those values that best fit the data illustrating various sources of water for plants that are defined by a range of soil depths. As the mixing model performs best when distinguishable 'sources' are used, we combined the soil water isotopic data into three soil layers according to the isotopic signatures and using the GWC–weighted mean approach, which was widely used in previous studies (Liu et al., 2014; Snyder and Williams, 2003; Zhang et al., 2017). Accordingly, stable isotope signatures of three potential water sources were considered as inputs in the Bayesian mixing model: (1) The shallow soil layer (0–20 cm) was sensitive to evaporation and precipitation pulse input, which has obvious seasonal patterns of isotopic values and SM; (2) The middle soil layer (20–40 cm) was mildly affected by precipitation and SM, and the variabilities of soil water isotopic compositions and SM were lower than the shallow soil layer; (3) The deep soil layer (40–100 cm) was less affected by precipitation and evaporation, and the variability of soil water isotopic compositions and SM of this soil layer were comparatively stable with the season and soil depths.

According to some latest studies, the water isotopes of plant xylem extracted by the low–temperature vacuum distillation method were not supposed to correctly reflect the δ^2H of water for transpiration (Chen et al., 2020a; De la Casa, 2022). However, the low–temperature vacuum distillation method is still the most popular plant extraction method due to the lack of an effective method to extract transpiration water directly, with more than 95 % of studies using this method according to a meta–analysis (De la Casa, 2022). To investigate the uncertainties of δ^2H deviation, this study used plant xylem water content to correct xylem water δ^2H according to Chen et al. (2020b) (the corrected xylem water δ^2H was 8.30 ‰ higher on average than the raw data). The RWU results from the two datasets presented few differences (equal to or less than 3 %, $p > 0.05$, Table 2). This finding was consistent with Evaristo et al. (2017), who found that a Bayesian mixing model with δ^2H and $\delta^{18}O$ was less sensitive to $^2H/^1H$ fractionation than the simple mass balance method, which could help to obtain more objective results. In summary, the average 8.30 % underestimation of δ^2H had no significant effect on the results of the plant water source in this study. Therefore, we used raw δ^2H and $\delta^{18}O$ as input data in the following analysis.

Relative contributions of different trees and shrubs to transpiration are not yet available, which makes it difficult to obtain the contributions of different soil layers to total transpiration at the ecosystem scale. Besides, no statistically significant difference was found in the water uptake fractions of coexisting plant species using one–way analysis of variance in most cases, except for the water uptake fractions of middle soil layer in the BF. The biomass of trees accounted for more than 97 % of the total biomass in the three forest ecosystems in our study region (Zhou, 2013). Landuyt et al. (2019) also found understory vegetation contributes 10 %–15 % of evapotranspiration in temperate forests with a dense canopy. Therefore, trees dominated in the forest ecosystems, and we chose to explore water uptake patterns of plants at the stand scale, and the mean weighted averages of water uptake fractions of trees were calculated using stand densities of trees as weights (the same process was performed for Figs. 6, 7 and 8), and the stand densities of trees in our study sites can be derived from Zhou (2013).

2.4. Niche overlap index

The 95 % credible interval of the proportional contribution of each source between two species was used to quantify the stand–level overlap of species as follows (Guo et al., 2018; Sepulveda et al., 2012):

$$\boldsymbol{O}_{\boldsymbol{AB,S}} = 2\frac{\boldsymbol{W}_{\boldsymbol{AB,S}}}{\boldsymbol{W}_{\boldsymbol{A,S}} + \boldsymbol{W}_{\boldsymbol{B,S}}} \quad (2)$$

where $\boldsymbol{W}_{\boldsymbol{A,S}}$ and $\boldsymbol{W}_{\boldsymbol{B,S}}$ are the widths of the 95 % credible interval of water uptake fractions for species A and B, respectively, $\boldsymbol{W}_{\boldsymbol{AB,S}}$ is the width of the intersection of 95 % credible interval of $\boldsymbol{W}_{\boldsymbol{A,S}}$ and $\boldsymbol{W}_{\boldsymbol{B,S}}$. $\boldsymbol{O}_{\boldsymbol{AB,S}}$ range from o to 1, and 0 indicates no overlap occurs and 1 indicates complete overlap. The number of species pairs are 1, 6 and 3 in BF, MF and CF, respectively.

2.5. Soil moisture determination

Soil water includes bound water and mobile water. Bound water refers to the water stored in the small pores of soil, including ineffective water and effective water (Petersen et al., 1996). The ineffective water is the part of water that below wilting coefficient, difficult for plants to use. The effective water refers to the part of water between wilting coefficient ($\boldsymbol{\theta}_w$, −1500 kPa) and the field capacity ($\boldsymbol{\theta}_{fc}$, −33 kPa), and it can be taken up by plants, which is defined as plant–available water (PAW) in

Table 2
Difference test of the water source contribution of different depth soil layers before and after the correction of δ^2H.

Sites	Tree species	Contributions of 0–20 cm soil (%)			Contributions of 20–40 cm soil (%)			Contributions of 40–100 cm soil (%)		
		CD	RD	*p* value	CD	RD	*p* value	CD	RD	*p* value
BF	*Lc*	39	39	0.94	28	27	0.82	3P3	34	0.98
	Df	35	34	0.85	34	33	0.55	31	33	0.65
MF	*Af*	31	32	0.93	34	33	0.46	34	35	0.78
	Pb	33	32	0.68	33	33	0.66	33	35	0.54
	Ac	38	37	0.77	31	31	0.94	31	32	0.76
	Ba	35	34	0.81	33	32	0.78	32	34	0.7
	Rp	32	30	0.33	33	33	0.7	35	38	0.24
CF	*Af*	35	32	0.65	27	28	0.81	38	40	0.75
	Sp	33	31	0.72	33	32	0.76	34	37	0.62
	Rp	33	32	0.87	28	29	0.89	39	40	0.94

Note: CD represents the proportions using corrected data, and RD represents the proportions using raw data.

this study. The part of soil water exceeding the θ_{fc} is called gravity water (GW) (Gardner, 1960). Volumetric soil moisture of the study sites was measured with soil moisture probes (ECH2O, Decagon Devices, USA) at 5 cm, 10 cm, 20 cm, and 40 cm with 30 min internals (Defined as VWC_1). However, the VWC_1 can only be derived from 0 to 40–cm soil. To explore the relationship between soil moisture components and RWU in the 0–100–cm soil, the values of GWC were transferred to volumetric soil moisture (Defined as VWC_2) using soil bulk density, which was measured by cutting ring method: Soil core samples ($n = 3$ for each depth) were collected by cutting rings with a volume of 100 cm^3, and then dried in an oven at 105 °C for 24 h to obtain soil bulk density (Wang et al., 2022). The average values of VWC_2 in the 0–40–cm soil fit well with that of VWC_1 (Fig. 3), with $R^2 = 0.76$, 0.86, and 0.88 for VWC_1 vs. VWC_2 in BF, MF, and CF, respectively, showing that VWC_2 can effectively represent volumetric soil water content in this study. Thus, VWC_2 were used to analyse the SM–RWU relationship.

Pressure plate apparatus (Bittelli and Flury, 2009; Kirkham, 2005) was used to measure soil water content under different water potentials, and then RETC (Van Genuchten et al., 1991) was used to fit water retention curves at different depths in this study. Therefore, the relative percentages of gravity water and plant–available water can be calculated as follows:

$$PAW = \begin{cases} VWC_2 - \theta_w, \ if \ VWC_2 < \theta_{fc} \\ \theta_{fc} - \theta_w, \ if \ VWC_2 \geq \theta_{fc} \end{cases} \quad (3)$$

$$GW = \begin{cases} 0, \ if \ VWC_2 < \theta_{fc} \\ VWC_2 - \theta_{fc}, \ if \ VWC_2 \geq \theta_{fc} \end{cases} \quad (4)$$

$$R_{GW} = \frac{GW}{GW + PAW} \times 100\% \quad (5)$$

$$R_{PAW} = \frac{PAW}{GW + PAW} \times 100\% \quad (6)$$

where θ_{fc} and θ_w were the field capacity and wilting point (%), respectively; R_{GW} (%) and R_{PAW} (%) were the relative percentages of gravity water and plant–available water, respectively.

2.6. Data analyses

One–way analysis of variance (ANOVA) was used to determine whether there were any statistically significant differences between water uptake fractions in different elevations or in different species. Linear–least square regression was used to analyse the linear relationships between water uptake fractions and soil moisture at different soil layers, and an F–test was adopted to explore whether the relationships were significant. All statistical analyses were performed in the R studio software (version 4.2.3), and all figures were drawn using R studio and OriginPro 2021 software.

3. Results

3.1. Seasonal changes in GWC

Soil moisture also differed significantly among sites and soil layers (Fig. 2b). The VWC_1 of BF was much less than that of CF and MF during the study period. In addition, the soil moisture in the 5–cm soil was greater than that of the 40–cm soil in BF and CF. The GWCs at different elevations also exhibited distinct seasonal and vertical variations (Fig. 4). The average GWCs were 27.16±10.61 % in BF, 41.43±13.83 % in MF, and 29.50±10.70 % in CF during the study periods. The GWC was the highest in MF while lowest in BF, and it decreased with soil depth. Additionally, there were noticeable seasonal changes in the soil moisture of the three forest ecosystems. While the deep soil moisture varied less with the season, the shallow soil layers (0–20 cm and 20–40 cm) exhibited substantially greater seasonal changes.

3.2. Seasonal water–use patterns of plants

The seasonal water sources of the tree species in the BF site are shown in Fig. 5a–b. *Lc* obtained the largest proportion of water from the shallow soil layer during the sampling periods, by 37.0 % and 40.0 % in 2018 and 2019, respectively, and the proportional contributions of the middle soil water were 29.4 % and 27.3 % from the middle soil and 33.6 % and 32.7 % from the deep soil in 2018 and 2019, respectively. The water uptake proportions of *Lc* showed pronounced differences among months. The lowest and highest contributions of shallow soil occurred in June (17.2 %) and August (62.6 %) in 2018, respectively. The proportions of water obtained from shallow soil and deep soil reached the largest proportions (57.6 % and 53.8 %) in September and July 2019, respectively. Compared to *Lc*, fewer differences existed among the proportions of water extracted by *Df* from different depths, and the water extracted from shallow soil also presented the largest proportions, by 35.1 % and 35.2 % for 2018 and 2019, respectively. Deep soil

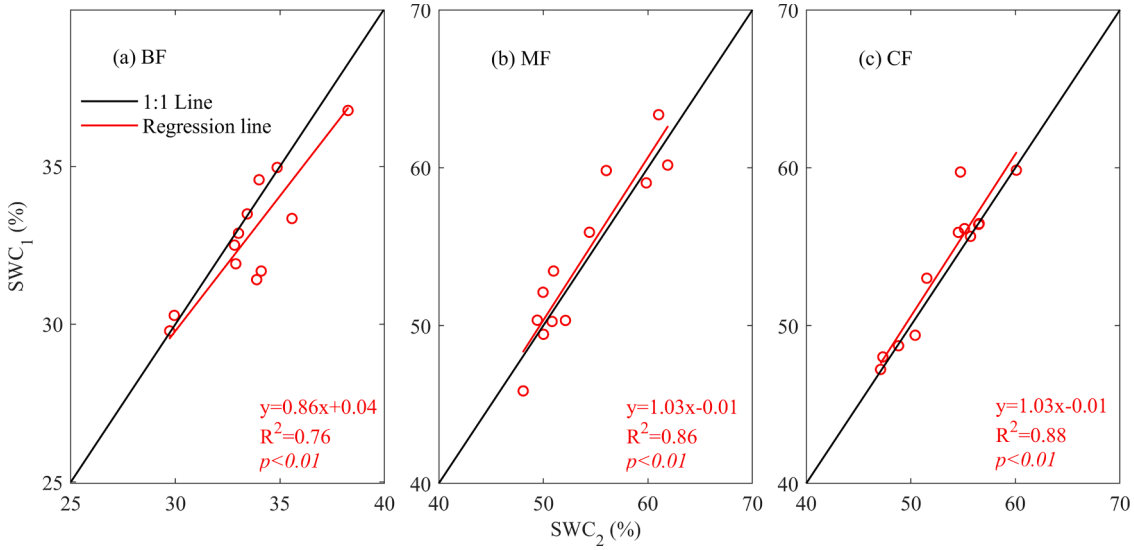

Fig. 3. Linear relationships between average volumetric soil moisture in 0–40 cm–soil measured by soil moisture probes (VWC_1) and volumetric soil moisture converted from gravimetric soil water content (VWC_2).

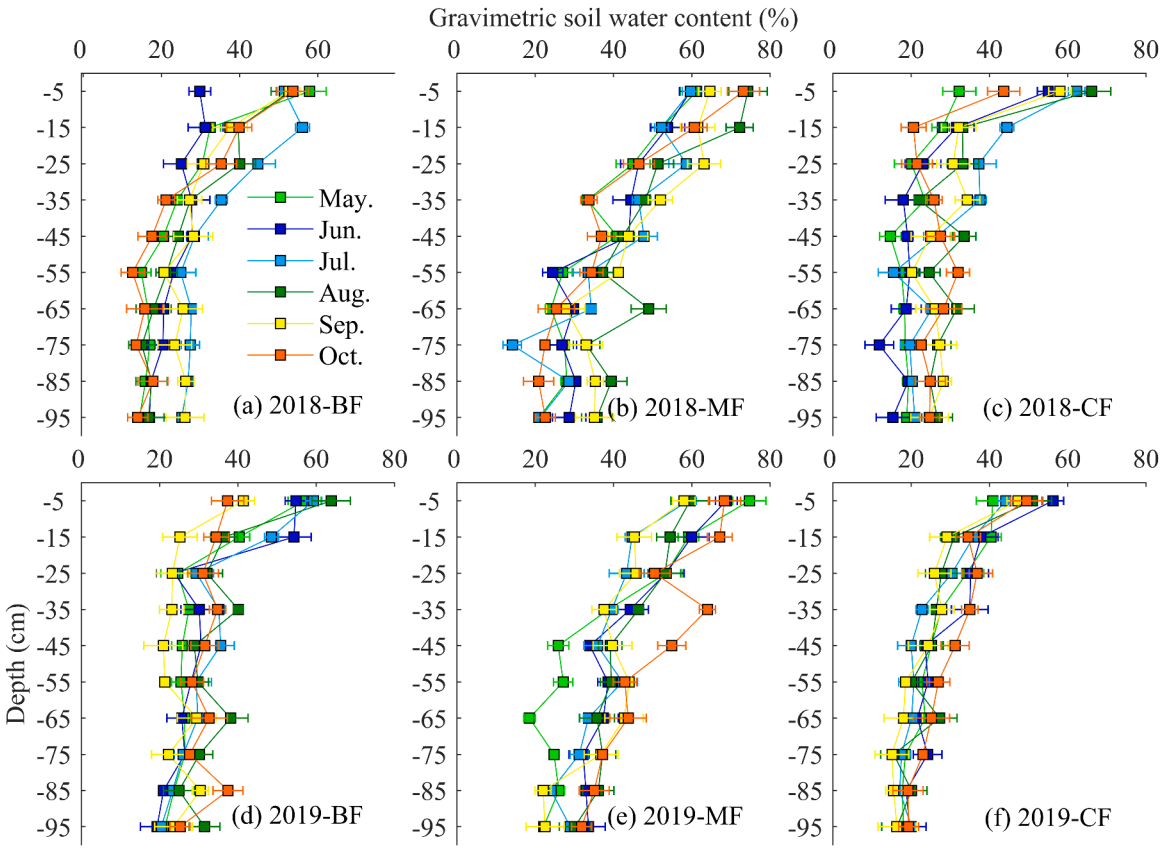

Fig. 4. Seasonal variation in gravimetric soil water content (%) at different depths in BF, MF, and CF. Error bars represent standard deviation.

contributed 30.3 % and 32.2 % of the obtained water in 2018 and 2019, whereas the middle soil contributed 34.5 % and 32.7 %, respectively. The highest contributions of shallow and deep soil layers existed in October (49.7 %) and June (44.4 %) in 2018, with 57.6 % and 53.8 % in September and July 2019, respectively.

The seasonal water sources of tree species in the MF site are shown in Fig. 5f–i. *Af* obtained 29.9 %, 34.4 %, and 35.8 % of its water from the shallow, middle, and deep soil moisture in 2018, respectively, with the largest proportion from the deep soil layer. However, similar proportions of water were provided by shallow, middle, and deep soil moisture in 2019 (33.1 %, 33.9 %, and 33.0 %, respectively), and few differences existed among seasons. Other tree species had similar water uptake patterns with *Af*. The proportions of water extracted by *Pb* were 34.5 % and 32.0 % from the shallow soil, 33.0 % and 33.8 % from the middle soil, and 32.5 % and 34.1 % from the deep soil in 2018 and 2019, respectively. The shallow soil contributed the largest percentage of water extracted by *Ac* both in 2018 and 2019 (40.9 % and 36.0 %, respectively), and the proportional contributions of middle and deep soil water obtained by *Ac* were close to 30 %. *Rp* obtained most of their water from shallow soil water (40.9 %) in 2018 and deep soil water (36.0 %) in 2019.

The seasonal water sources of the tree species in the CF site are shown in Fig. 5c–e. *Af, Sp and Rp* obtained the largest proportions of soil water from the deep and shallow soil layers in 2018 (43.9 %, 40.3 %, and 48.1 %) and 2019 (39.3 %, 38.2 %, and 37.3 %), respectively. The three tree species had similar water uptake patterns during the sampling periods.

3.3. Relationship between root water uptake and soil moisture components

Water uptake fractions of the major tree species were related to VWC_2 at different depths in linear regressions (Fig. 6). In most cases, plants showed significant trends of decreasing proportions of soil water uptake from the upper soil layers (0–20 cm and 20–40 cm) and increasing proportions of soil water from the deep soil layer (40–100 cm) when the soil moisture increased at the stand scale. In the BF and CF sites, water uptake fractions showed significant negative trends ($p<0.05$) with soil moisture of shallow and middle soil layers, while significant positive trends ($p<0.05$) were found in the deep soil layer. In the MF site, significant negative and positive trends ($p<0.05$) between water uptake fractions and soil water content were also found in the shallow and deep soil layers, respectively.

To further explore the relationship between the compositions of soil water and plant water uptake, sampling campaigns were divided into Group I and Group II based on the proportional water sources of different soil layers. Owing to the reason that water uptake fractions from the middle soil layer had relatively fewer fluctuations, only shallow and deep soil layers were examined. Sampling campaigns were divided into Group I once the fraction of shallow soil water was greater than that of deep soil water, while sampling campaigns were divided into Group II once the fraction of deep soil water was greater than that of shallow soil water.

For BF, plants in Group I obtained 52 % and 19 % of their water from shallow soil and deep soil, respectively, while plants in Group II obtained 19 % and 49 % of their water from shallow soil and deep soil, respectively (Fig. 7). However, the relative proportions of gravity water (R_{GW}) and plant–available water (R_{PAW}) of the 0–20–cm soil in Group I were 33 % and 66 %, respectively, and they were 43 % and 57 % in Group II. Compared to Group II, Group I had a larger proportion of plant–available water and a smaller proportion of gravity water in the shallow soil layer. R_{GW} and R_{PAW} of the 40–100 cm soil in Group I were 0 and 100 %, respectively, and they were 3 % and 97 % in Group II. For MF, the proportional contributions of shallow and deep soil layers in

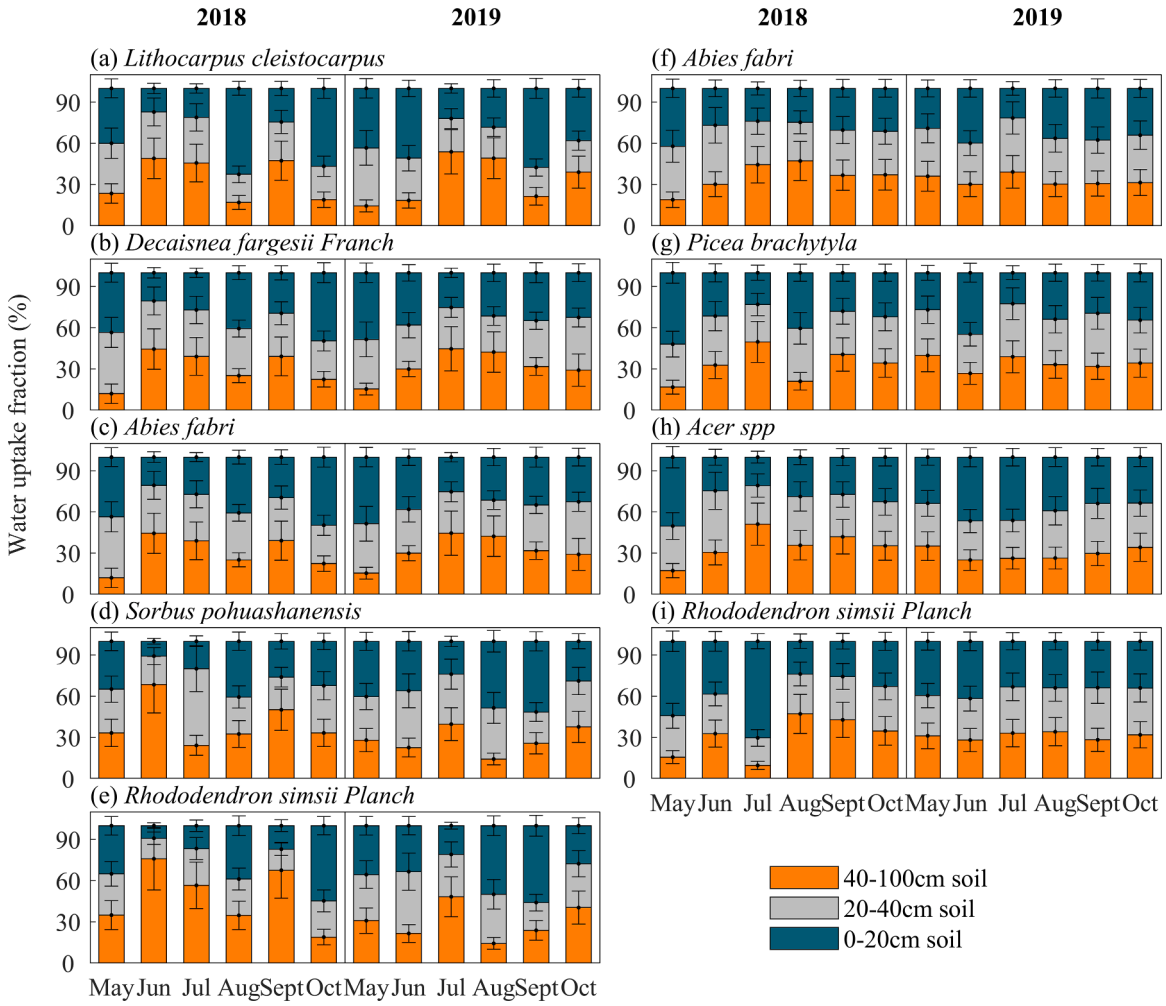

Fig. 5. Water sources of dominant tree species in the (a–b) broad–leaved forest, (f–i) the coniferous and broad–leaved mixed forest, and (c–e) the coniferous forest. Error bars represent standard deviation.

Group I were 38 % and 28 %, and the values for Group II were 27 % and 39 %, respectively. The percentages of gravity water and plant–available water were 39 % and 61 %, respectively, for Group I and 46 % and 53 %, respectively, for Group II. R_{GW} and R_{PAW} of the 40–100 cm soil were 99% and 1 %, respectively, both in Group I and Group II. A similar pattern was also found in CF. The water uptake proportions from shallow soil were 46 % and 21 %, with 21 % and 54 % from deep soil for Group I and Group II, respectively. However, the relative proportions of gravity water 0–20–cm soil were 33 % and 43 %, respectively, and those of plant–available water were 67 % and 57 % for Group I and Group II, respectively. R_{GW} of the 40–100 cm soil was 0 %, and R_{PAW} of 40–100 cm was 100 %. These findings affirm the concurrent occurrence of higher water uptake fractions and greater proportions of plant-available water in the shallow soil within the study region.

Moreover, a comparison between 2018 and 2019 demonstrates that plants in the three forest stands utilized a greater proportion of shallow soil water in 2019 (significant at $p< 0.05$ in BF and CF). This trend was also consistent with larger proportions of plant–available water in 2019 (Fig. 8).

4. Discussion

4.1. Variations of root plant water uptake patterns among species

Our results reveal that both trees and shrubs shared comparable water sources within the same habitants, with no significant differences found in water uptake fractions among coexisting species along the elevational gradient (Fig. 5). The values of pairwise niche overlap also affirmed substantial overlaps of water sources among coexisting species (Fig. 9). In three sites, the values for 0–20 cm soil and 40–100 cm soil are greater than 0.71 and 0.82 (Fig. 9), respectively. This observation contradicts the findings of some previous studies, which suggested that coexisting species might exhibit complementary niches in utilizing soil water, resulting in hydrological niche segregation (Chi et al., 2019; Martorell et al., 2015; Muñoz-Villers et al., 2020; O'Keefe et al., 2019). This inconsistency could be attributed to variations in water conditions. Notably, niche segregation in water–limited areas can help plants avoid competition and withstand drought stress—an adaptation that may not be necessary for plants in humid regions (del Castillo et al., 2016). Our findings confirm the classical niche partitioning theory, demonstrating that water source niche overlap increases with water availability (Guo et al., 2018), and plants tend to exhibit larger overlaps of water sources when water availability is not restricted (Connell, 1978).

4.2. Soil water components control temporal plant water uptake patterns

Across all sites in this study, a negative relationship between soil moisture and water uptake fractions was observed in the shallow soil, while soil moisture displayed a positive correlation with water uptake fractions in the soil 40 cm (Fig. 6). This suggests that as soil moisture levels increase, plants tend to shift their water uptake to deeper soil layers. This outcome challenges the conventional notion that plants

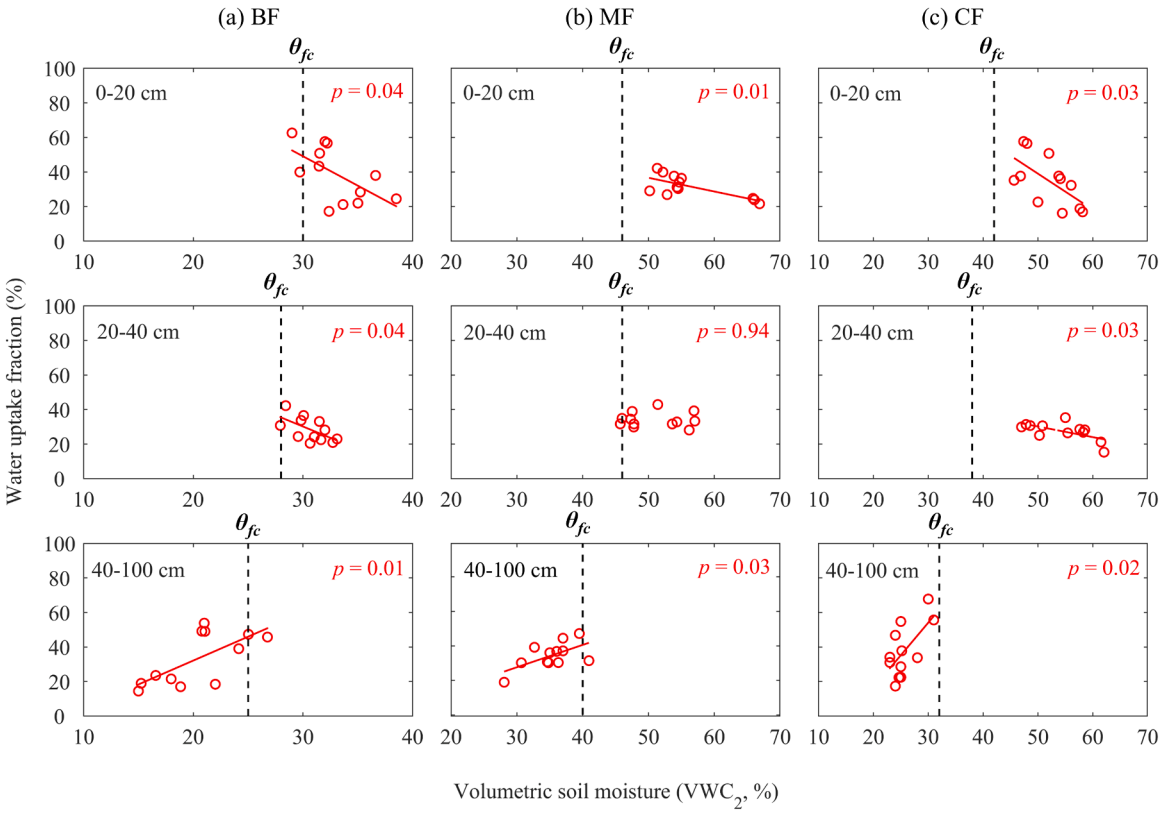

Fig. 6. Linear relationships between the proportional water uptake of different soil layers and soil moisture at the stand scale. Black dotted line refers to the field capacity.

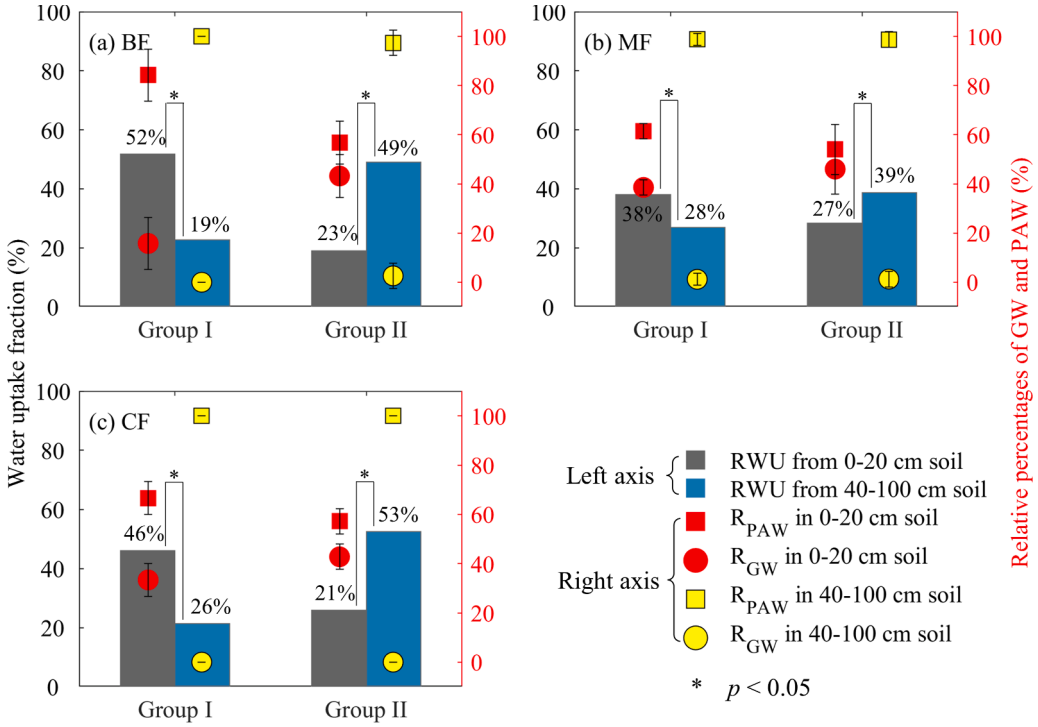

Fig. 7. Water uptake fractions, average percentages of gravity water and plant–available water of 0–20 cm soil and 40–100 cm soil in Group I and Group II.

primarily utilize shallow soil water when surface soil water is abundant (Brinkmann et al., 2018; Dawson and Pate, 1996; Grossiord et al., 2019). The use of shallow soil water enables plants to access nutrient–rich zones concentrated within the 0–20 cm soil layer (Jobbágy and Jackson, 2001) and explains the prevalence of root systems for temperate forest tree species in the upper soil layer (Meinen et al., 2009). With decreasing soil

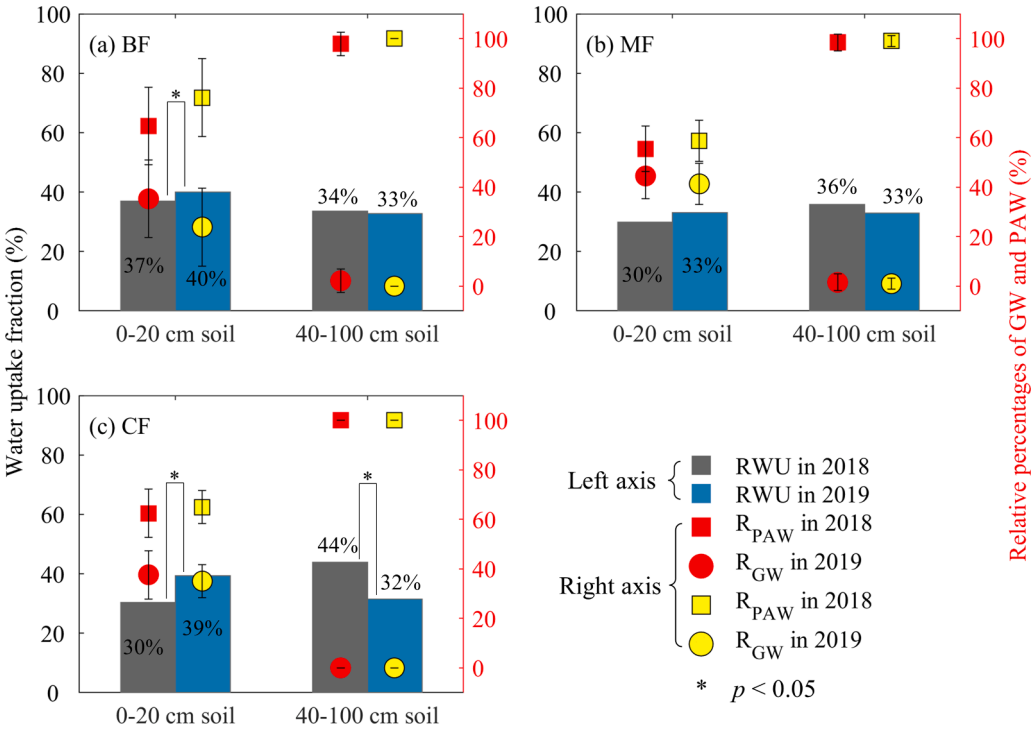

Fig. 8. Water uptake fractions, average percentages of gravity water and plant–available water of 0–20 cm soil and 40–100 cm soil in 2018 and 2019.

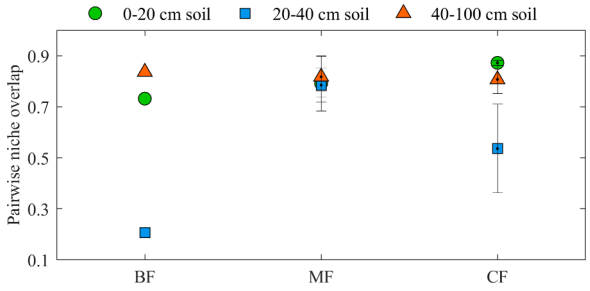

Fig. 9. Pairwise niche overlap of each source along the elevational gradient. It's worth noting that values of niche overlap in BF site lacks error bars due to the presence of only one species pair.

moisture, leading to more negative soil matrix potentials, plants are compelled to tap into deeper soil layers for sustaining their vital physiological processes (Brinkmann et al., 2018), thus yielding a positive SM–RWU relationship in the shallow soil (Brinkmann et al., 2019).

This discrepancy in the SM–RWU relationship observed in this study compared to previous researches could also stem from differing habitat water conditions. Our findings reveal that a higher proportion of gravity water within the 0–20 cm soil layer consistently co–occurs with a lower water uptake fraction from the same soil layer across the three forest stands (Fig. 7). This phenomenon may be attributed to the poor aeration resulting from excessive soil water in the shallow soil. This poor aeration is substantiated by soil moisture levels in the 0–20 cm depth exceeding $\boldsymbol{\theta}_{fc}$ at most sampling campaigns, indicating compromised oxygen availability in the shallow soil. Specifically, the larger pores in the upper soil layers become progressively inundated with gravitational water due to precipitation replenishment, leading to reduced oxygen content. The deleterious impact of excessive water on plant growth finds support in previous studies conducted in agroecosystems and forests (Pezeshki, 2001; Zaidi et al., 2007). Poor aeration may result impeding root respiration and root pressure (Nobel, 2003; Ouyang and Boersma, 1992), subsequently influence the root water absorbability. For example, *T. distichum* lived in coastal delta tend to absorb shallow soil water with better aeration instead of deep soils (Zhang et al., 2021).

Additionally, in this study, the disparities in water sources and soil water components between a normal year and a wet year (Fig. 8) further illuminate the influence of soil water components on plant water uptake dynamics in extremely humid regions.

4.3. Water uptake strategies along the elevational gradient

Climatic variables always exhibit elevational–dependency, which can exert substantial influence on hydrological processes as elevation rises (Gentile et al., 2023; Körner and Cochrane, 1985; Yang et al., 2019). As reported in our previous study, precipitation (P) increases with elevation in the forest region on the eastern edge of Mount Gongga, while evapotranspiration (ET) decreases with elevation, resulting from a decrease in energy condition (Hu et al., 2023; Sun et al., 2020). Increasing P and decreasing ET along the elevational gradient led to an increase of available water (P-ET) along the elevational gradient, which may subsequently result in higher soil saturation at higher elevations compared to lower elevations on the eastern edge of Mount Gongga. We identified distinct water uptake strategies along the elevational gradient (Table 3). One–way ANOVA analysis disclosed a noteworthy disparity ($p< 0.05$) in water uptake fractions between BF and the other two sites, both in shallow and deep soils. Specifically, trees in BF exhibited a greater reliance on shallow soil water (38.5 %) and a lesser dependence on deep soil water compared to those in MF and CF (31.3% vs. 34.9 %). This result diverges from a previous study in a drought–prone Douglas fir forest, where trees at lower elevations with lower precipitation levels extracted more deep soil water originating from winter precipitation (Martin et al., 2018).

The variations of soil water components in the surface soil are consistent with the different elevational patterns of plant water uptake, showing a larger proportion of PAW in BF compared to MF and CF. While soil water components undeniably shape the seasonal dynamics of water sources, the question of whether elevational differences in plant water uptake are driven by water availability or tree species remains unanswered. Given that the fine root is a main organ for water

Table 3
Proportional contributions of water sources and relative percentages of gravity water and plant–available water at the stand scale.

Soil layers	BF			MF			CF		
	RWU	GW	PAW	RWU	GW	PAW	RWU	GW	PAW
Shallow	38.5 %^{b}	29.6 %^{b}	70.4 %^{b}	31.5 %^{a,c}	42.9 %^{a,c}	57.1 %^{a,c}	34.9 %^{b}	36.3 %^{b}	63.7 %^{b}
Middle	28.3 %^{b}	42.5 %^{b,c}	57.5 %^{b,c}	34.1 %^{a,c}	29.1 %^{a,c}	70.9 %^{a,c}	27.5 %^{b}	53.3 %^{a,b}	46.7 %^{a,b}
Deep	33.1 %^{c}	1.1 %	98.9 %	34.4 %	1.3 %	98.7 %	37.7 %^{a}	0	100 %

Note: a, b, and c represent statistically significant differences between the variable and those in BF, MF, and CF, respectively.

absorption, to address this query, we conducted an analysis of root distribution in both BF and CF. Prior research has indicated that tree species with deeper–rooted profiles tend to extract water from deeper soil layers (Gessler et al., 2022; Leuzinger et al., 2005; Zapater et al., 2013). Our findings reveal that fine roots were predominantly distributed within the 0–40 cm soil layer for both BF (93 %) and CF (91 %) (Table 4). This finding underscores that the fine root systems of both sites are concentrated within the 0–40 cm soil depth. Therefore, no compelling evidence supports the notion that the seasonal and elevational patterns of root water uptake are attributable to variations in root distribution. Besides, both trees and shrubs are included in the three sites, encompassing a variety of growth characteristics, such as differences in breast diameter and tree height. However, our investigation discerns substantial overlaps in water sources across all forest sites, implying a parallelism in water uptake strategies among diverse species. This robust finding attests to the relatively minor discrepancies in water uptake approaches exhibited by various species within the humid subalpine region. Due to the above analysis, we can conclude that it is water availability control the patterns of root water uptake along the elevational gradient of Mount Gongga.

4.4. Implications

Precipitation and air temperature showed decreasing and increasing trends (Fig. 2), and an anticipated rise in evapotranspiration is projected in the study area (Hu et al., 2023), indicating an impending shift toward heightened aridity and elevated temperatures in the area. This shift will inherently lead to diminished water availability within the forest ecosystems. In the context of climate change, the dynamics of plant water uptake patterns could undergo transformation. On one hand, reduced precipitation and amplified evapotranspiration at lower elevations could initially subject species inhabiting these regions to seasonal drought due to decreased precipitation (Panthi et al., 2020; Shi et al., 2021). The water availability decrease could trigger competition for shallow soil water resources, thereby impacting plant growth. However, it's important to acknowledge that this trend may cease as soil moisture levels fall below $\boldsymbol{\theta_{fc}}$. On the other hand, due to larger decrease of precipitation was found in higher elevations (Hu, 2018), more pronounced decreases in water availability are expected at higher elevations compared to lower ones, consequently further attenuating the elevational patterns of plant water uptake. Notably, excessive soil moisture in humid areas can impede plant root growth due to inadequate aeration and soil anaerobiosis. Management practices that enhance soil aeration conditions in humid areas, such as avoiding compaction and implementing effective drainage, could significantly promote root growth and enhance overall plant health (Pezeshki, 2001).

In future research, the previously unreported negative SM–RWU relationship in the shallow soil layer should be further validated in more humid ecosystems. Leveraging a combination of high–frequency isotopic tracing and advanced root system monitoring techniques offers the potential for deeper insights into the dynamic interplay between plants' RWU and soil water dynamics. Besides, soil properties wield significant influence over soil water content, subsequently impacting plant water uptake dynamics. For instance, finer soil textures possess greater water–holding capacities, explaining the higher soil water content observed in regions with lower precipitation, such as MF in comparison to CF. As such, forthcoming research endeavors must incorporate these variations in soil properties, particularly in mountainous regions characterized by substantial spatial soil heterogeneity.

Table 4
Root biomass (g/m$^{3)}$ of different soil layers.

Soil layers	BF		CF	
	Total	Fine roots	Total	Fine roots
0–40 cm	215.33±12.47	93.91±12.51	110.33±10.78	67.32±10.87
40–100 cm	17.50±4.50	7.44±1.30	16.00±4.15	6.37±1.23

5. Conclusion

We reported the seasonal water uptake patterns of dominant species along a subalpine elevation gradient on Mount Gongga, situated at the eastern edge of the Qinghai–Tibet Plateau. Our results demonstrate that hydrological niche segregation among species did not occur within humid ecosystems. Negative and positive relationships can be found between soil moisture and water uptake fractions in the shallow and deep soil layers, respectively. This water uptake pattern is related to the soil water compositions, and soil water adjusts water uptake patterns in a way that is different from that in arid regions. The relative proportion of gravity water in the shallow soil rose as soil moisture increased, which can affect soil aeration and subsequently restrain root activities, and increase soil moisture supply in deep soil by plant–available water. Therefore, plants tended to shift their water uptake to deep soil with increasing soil moisture. In addition, at the stand scale, plants used more deep soil water and less shallow soil water with increasing elevation. Compared to MF and CF, plants in BF at the low altitude with lower soil moisture obtained more shallow soil water, which can also support our understanding of how soil moisture components affect water–use strategies.

CRediT authorship contribution statement

Juying Sun: Conceptualization, Investigation, Methodology, Visualization, Writing – original draft, Writing – review & editing. **Xiangyang Sun:** Conceptualization, Funding acquisition, Methodology, Writing – review & editing. **Genxu Wang:** Conceptualization, Funding acquisition, Methodology, Resources, Writing – review & editing. **Wenchang Dong:** Data curation, Investigation, Writing – review & editing. **Zhaoyong Hu:** Supervision, Writing – review & editing. **Shouqin Sun:** Funding acquisition, Supervision, Writing – review & editing. **Fei Wang:** Data curation, Investigation. **Chunlin Song:** Data curation, Writing – review & editing. **Shan Lin:** Data curation, Writing – review & editing.

Declaration of Competing Interest

The authors declare that they have no known competing financial interests or personal relationships that could have appeared to influence the work reported in this paper.

Data availability

Data will be made available on request.

Acknowledgments

This research was supported by the Strategic Priority Research Program of the Chinese Academy of Sciences (Grant No. XDA23090201), the National Natural Science Foundation of China (Grant No. 42330508 and No. 41977176), Science & Technology Fundamental Resources Investigation Program (Grant No.2022FY100205), Specialized Postdoctoral Research and Development Fund of Sichuan University (Grant No. 2023SCU12118) and the Science and Technology Project of Sichuan Province (Grant No. 2022NSFSC1001).

References

Berry, Z.C., Hughes, N.M., Smith, W.K., 2014. Cloud immersion: an important water source for spruce and fir saplings in the Southern Appalachian Mountains. Oecologia 174 (2), 319–326.
Beyer, M., Hamutoko, J., Wanke, H., Gaj, M., Koeniger, P., 2018. Examination of deep root water uptake using anomalies of soil water stable isotopes, depth-controlled isotopic labeling and mixing models. J. Hydrol. 566, 122–136. Amst.
Bittelli, M., Flury, M., 2009. Errors in water retention curves determined with pressure plates. Soil Sci. Soc. Am. J. 73 (5), 1453–1460.
Brinkmann, N., Eugster, W., Buchmann, N., Kahmen, A., 2019. Species-specific differences in water uptake depth of mature temperate trees vary with water availability in the soil. Plant Biol. 21 (1), 71–81.
Brinkmann, N., et al., 2018. Employing stable isotopes to determine the residence times of soil water and the temporal origin of water taken up by Fagus sylvatica and Picea abies in a temperate forest. New Phytol. 219 (4), 1300–1313.
Capelli, A., et al., 2022. GNSS signal-based snow water equivalent determination for different snowpack conditions along a steep elevation gradient. Cryosphere 16 (2), 505–531.
Chen, Y., et al., 2020a. Stem water cryogenic extraction biases estimation in deuterium isotope composition of plant source water. Proc. Natl. Acad. Sci. U. S. A. 117 (52), 33345–33350.
Chen, Y., et al., 2020b. Stem water cryogenic extraction biases estimation in deuterium isotope composition of plant source water. Proc. Natl. Acad. Sci. 117 (52), 33345–33350.
Cheng, X., et al., 2006. Summer rain pulse size and rainwater uptake by three dominant desert plants in a desertified grassland ecosystem in northwestern China. Plant Ecol. 184 (1), 1–12.
Chi, Y., Zhou, L., Yang, Q., Li, S.P., Zheng, S., 2019. Increased snowfall weakens complementarity of summer water use by different plant functional groups. Ecol. Evol. 9 (7), 4264–4274.
Connell, J.H., 1978. Diversity in tropical rain forests and coral reefs: high diversity of trees and corals is maintained only in a nonequilibrium state. Science 199 (4335), 1302–1310.
Dash, S.S.S., et al., 2022. Biochemical characterization of maize (Zea mays L.) hybrids under excessive soil moisture stress. Cereal Res. Commun. 50 (4), 875–884.
Dawson, T.E., Mambelli, S., Plamboeck, A.H., Templer, P.H., Tu, K.P., 2002. Stable isotopes in plant ecology. u. Rev. Ecol. Syst. 33 (1), 507–559.
Dawson, T.E., Pate, J.S., 1996. Seasonal water uptake and movement in root systems of Australian phraeatophytic plants of dimorphic root morphology: a stable isotope investigation. Oecologia 107 (1), 13–20.
De la Casa, J., et al., 2022. Isotopic offsets between bulk plant water and its sources are larger in cool and wet environments. Hydrol. Earth Syst. Sci. 26 (15), 4125–4146.
del Castillo, J., Comas, C., Voltas, J., Ferrio, J.P., 2016. Dynamics of competition over water in a mixed oak-pine Mediterranean forest: spatio-temporal and physiological components. For. Ecol. Manag. 382, 214–224.
Della Chiesa, S., et al., 2014. Modelling changes in grassland hydrological cycling along an elevational gradient in the Alps. Ecohydrology 7 (6), 1453–1473.
Ellsworth, P.Z., Sternberg, L.S., 2015. Seasonal water use by deciduous and evergreen woody species in a scrub community is based on water availability and root distribution. Ecohydrology 8 (4), 538–551.
Evaristo, J., McDonnell, J.J., Clemens, J., 2017. Plant source water apportionment using stable isotopes: a comparison of simple linear, two-compartment mixing model approaches. Hydrol. Process. 31 (21), 3750–3758.
Feng, J., Tang, M., Zhu, B., 2021. Soil priming effect and its responses to nutrient addition along a tropical forest elevation gradient. Glob. Change Biol. 27 (12), 2793–2806.
Gardner, W.R., 1960. Dynamic aspects of water availability to plants. Soil Sci. 89 (2), 63–73.
Gentile, A., et al., 2023. Towards a conceptualization of the hydrological processes behind changes of young water fraction with elevation: a focus on mountainous alpine catchments. Hydrol. Earth Syst. Sci. 27 (12), 2301–2323.
Gessler, A., et al., 2022. Drought reduces water uptake in beech from the drying topsoil, but no compensatory uptake occurs from deeper soil layers. New Phytol. 233 (1), 194–206.
Good, S.P., Noone, D., Bowen, G., 2015. Hydrologic connectivity constrains partitioning of global terrestrial water fluxes. Science 349 (6244), 175–177.
Goulden, M., et al., 2012. Evapotranspiration along an elevation gradient in California's Sierra Nevada. Journal of Geophysical Research: Biogeosciences 117 (G3).
Grossiord, C., et al., 2019. Prolonged warming and drought modify belowground interactions for water among coexisting plants. Tree Physiol. 39 (1), 55–63.
Guo, J.S., Hungate, B.A., Kolb, T.E., Koch, G.W., 2018. Water source niche overlap increases with site moisture availability in woody perennials. Plant Ecol. 219 (6), 719–735.
Hu, Z., 2018. Estimation of Evapotranspiration in Different Forest Types Based On the Relationship between Water and Carbon on the Eastern Slope of Mount Gongga. University of Chinese Academy of Sciences.
Hu, Z., et al., 2023. Controlling Factors of the Spatial-Temporal Fluctuations in Evapotranspiration Along an Elevation Gradient Across Humid Montane Ecosystems. Water Resour. Res. 59 (1), e2022WR033228.
Hu, Z., et al., 2018. Spatial-temporal patterns of evapotranspiration along an elevation gradient on Mount Gongga, Southwest China. Water Resour. Res. 54 (6), 4180–4192.
Jing, C.Q., Li, L., Chen, X., Luo, G.P., 2014. Comparison of root water uptake functions to simulate surface energy fluxes within a deep-rooted desert shrub ecosystem. Hydrol Process 28 (21), 5436–5449.
Jobbágy, E.G., Jackson, R.B., 2001. The distribution of soil nutrients with depth: global patterns and the imprint of plants. Biogeochemistry 53 (1), 51–77.
Juhlke, T.R., et al., 2021. Temporal offset between precipitation and water uptake of Mediterranean pine trees varies with elevation and season. Sci. Total Environ. 755, 142539.
Jung, E.Y., et al., 2014. Influence of elevation on canopy transpiration of temperate deciduous forests in a complex mountainous terrain of South Korea. Plant Soil 378 (1–2), 153–172.
Kirkham, M., 2005. Field capacity, wilting point, available water, and the non-limiting water range. Princ. Soil Plant Water Relat. 8, 101–115.
Köcher, P., Horna, V., Beckmeyer, I., Leuschner, C., 2012. Hydraulic properties and embolism in small-diameter roots of five temperate broad-leaved tree species with contrasting drought tolerance. Ann. For. Sci. 69 (6), 693–703.
Körner, C., Cochrane, P., 1985. Stomatal responses and water relations of eucalyptus pauciflora in summer along an elevational gradient. Oecologia 66, 443–455.
Landuyt, D., et al., 2019. The functional role of temperate forest understorey vegetation in a changing world. Glob. Change Biol. 25 (11), 3625–3641.
Leuzinger, S., Zotz, G., Asshoff, R., Körner, C., 2005. Responses of deciduous forest trees to severe drought in Central Europe. Tree Physiol. 25 (6), 641–650.
Li, Y., Fuchs, M., Cohen, S., Cohen, Y., Wallach, R., 2002. Water uptake profile response of corn to soil moisture depletion. Plant Cell Environ. 25 (4), 491–500.
Li, Y., Niu, W., Zhang, M., Wang, J., Zhang, Z., 2020. Artificial soil aeration increases soil bacterial diversity and tomato root performance under greenhouse conditions. Land Degrad. Dev. 31 (12), 1443–1461.
Lian, X., et al., 2018. Partitioning global land evapotranspiration using CMIP5 models constrained by observations. Nat. Clim. Change 8 (7), 640–646.
Liu, J., et al., 2021. Using stable isotopes to quantify root water uptake under a new planting pattern of high-low seed beds cultivation in winter wheat. Soil Tillage Res. 205, 104816.
Liu, W., Wang, P., Li, J., Liu, W., Li, H., 2014. Plasticity of source-water acquisition in epiphytic, transitional and terrestrial growth phases of Ficus tinctoria. Ecohydrology 7 (6), 1524–1533.
Liu, Z., Yu, X., Jia, G., 2019. Water uptake by coniferous and broad-leaved forest in a rocky mountainous area of northern China. Agric. For. Meteorol. 265, 381–389.
Ma, Y.J., et al., 2019. Evapotranspiration and its dominant controls along an elevation gradient in the Qinghai Lake watershed, Northeast Qinghai-Tibet Plateau. J. Hydrol. 575, 257–268. Amst.
Martin, J., Looker, N., Hoylman, Z., Jencso, K., Hu, J., 2018. Differential use of winter precipitation by upper and lower elevation Douglas fir in the Northern Rockies. Glob. Change Biol. 24 (12), 5607–5621.
Martorell, C., Almanza-Celis, C.A., Pérez-García, E.A., Sánchez-Ken, J.G., 2015. Co-existence in a species-rich grassland: competition, facilitation and niche structure over a soil depth gradient. J. Veg. Sci. 26 (4), 674–685.
Meinen, C., Leuschner, C., Ryan, N.T., Hertel, D., 2009. No evidence of spatial root system segregation and elevated fine root biomass in multi-species temperate broad-leaved forests. Trees 23 (5), 941–950.
Muñoz-Villers, L.E., Geris, J., Alvarado-Barrientos, M.S., Holwerda, F., Dawson, T., 2020. Coffee and shade trees show complementary use of soil water in a traditional agroforestry ecosystem. Hydrol. Earth Syst. Sci. 24 (4), 1649–1668.
Musselman, K.N., Molotch, N.P., Margulis, S.A., 2017. Snowmelt response to simulated warming across a large elevation gradient, southern Sierra Nevada, California. Cryosphere 11 (6), 2847–2866.
Nandy, S., Saranya, M., Srinet, R., 2022. Spatio-temporal variability of water use efficiency and its drivers in major forest formations in India. Remote Sens. Environ. 269, 112791.
Nobel, P.S., 2003. Environmental Biology of Agaves and Cacti. Cambridge University Press.
O'Keefe, K., Nippert, J.B., McCulloh, K.A., 2019. Plant water uptake along a diversity gradient provides evidence for complementarity in hydrological niches. Oikos 128 (12), 1748–1760.
Ouyang, Y., Boersma, L., 1992. Dynamic oxygen and carbon dioxide exchange between soil and atmosphere: I. Model development. Soil Sci. Soc. Am. J. 56 (6), 1695–1702.
Panthi, S., Fan, Z.X., van der Sleen, P., Zuidema, P.A., 2020. Long-term physiological and growth responses of Himalayan fir to environmental change are mediated by mean climate. Glob. Change Biol. 26 (3), 1778–1794.

Parnell, A. and Inger, R., 2016. Stable isotope mixing models in R with simmr. URL https://cran.r-project.org/web/packages/simmr/vignettes/simmr.html.
Penna, D., Geris, J., Hopp, L., Scandellari, F., 2020. Water sources for root water uptake: using stable isotopes of hydrogen and oxygen as a research tool in agricultural and agroforestry systems. Agric. Ecosyst. Environ. 291, 106790.
Peters, A., Durner, W., Iden, S.C., 2017. Modified Feddes type stress reduction function for modeling root water uptake: accounting for limited aeration and low water potential. Agric. Water Manag. 185, 126–136.
Petersen, L.W., Moldrup, P., Jacobsen, O.H., Rolston, D.E., 1996. Relations between specific surface area and soil physical and chemical properties. Soil Sci. 161 (1), 9–21.
Pezeshki, S., 2001. Wetland plant responses to soil flooding. Environ. Exp. Bot. 46 (3), 299–312.
Rossatto, D.R., de Carvalho Ramos Silva, L., Villalobos-Vega, R., Sternberg, L.d.S.L., Franco, A.C., 2012. Depth of water uptake in woody plants relates to groundwater level and vegetation structure along a topographic gradient in a neotropical savanna. Environ. Exp. Bot. 77, 259–266.
Sajedi, T., Prescott, C.E., Seely, B., Lavkulich, L.M., 2012. Relationships among soil moisture, aeration and plant communities in natural and harvested coniferous forests in coastal British Columbia, Canada. J. Ecol. 100 (3), 605–618.
Schultz, N.M., Griffis, T.J., Lee, X., Baker, J.M., 2011. Identification and correction of spectral contamination in 2H/1H and 18O/16O measured in leaf, stem, and soil water. Rapid Commun. Mass Spectrom. 25 (21), 3360–3368.
Sepulveda, A.J., Lowe, W.H., Marra, P.P., 2012. Using stable isotopes to test for trophic niche partitioning: a case study with stream salamanders and fish. Freshw. Biol. 57 (7), 1399–1409.
Shi, S., Liu, G., Li, Z., Ye, X., 2021. Elevation-dependent growth trends of forests as affected by climate warming in the Southeastern Tibetan Plateau. For. Ecol. Manag. 498, 119551.
Silvertown, J., Araya, Y., Gowing, D., 2015. Hydrological niches in terrestrial plant communities: a review. J. Ecol. 103 (1), 93–108.
Snyder, K., Williams, D., 2003. Defoliation alters water uptake by deep and shallow roots of Prosopis velutina (Velvet Mesquite). Funct. Ecol. 17 (3), 363–374.
Sprenger, M., Leistert, H., Gimbel, K., Weiler, M., 2016. Illuminating hydrological processes at the soil-vegetation-atmosphere interface with water stable isotopes. Rev. Geophys. 54 (3), 674–704.
Sun, J.Y., Sun, X.Y., Hu, Z.Y., Wang, G.X., 2020. Exploring the influence of environmental factors in partitioning evapotranspiration along an elevation gradient on Mount Gongga, Eastern edge of the Qinghai-Tibet Platea, China. J. Mt. Sci. 17 (2), 384–396.
Thomas, A., Yadav, B.K., Šimůnek, J., 2020. Root water uptake under heterogeneous soil moisture conditions: an experimental study for unraveling compensatory root water uptake and hydraulic redistribution. Plant Soil 457 (1), 421–435.
van den Bergh, T., Inauen, N., Hiltbrunner, E., Körner, C., 2013. Climate and plant cover co-determine the elevational reduction in evapotranspiration in the Swiss Alps. J. Hydrol. 500, 75–83. Amst.
Van Genuchten, M.v., Leij, F. and Yates, S., 1991. The RETC code for quantifying the hydraulic functions of unsaturated soils.
Vetaas, O.R., Paudel, K.P., Christensen, M., 2019. Principal factors controlling biodiversity along an elevation gradient: water, energy and their interaction. J. Biogeogr. 46 (8), 1652–1663.
Vitasse, Y., et al., 2021. Phenological and elevational shifts of plants, animals and fungi under climate change in the European Alps. Biol. Rev. 96 (5), 1816–1835.
Wang, F., et al., 2022. Preferential flow patterns in forested hillslopes of the east Tibetan Plateau revealed by dye tracing and soil moisture network. Eur. J. Soil Sci. 73 (4), e13294.
Wang, H., Li, X., Xiao, J., Ma, M., 2021. Evapotranspiration components and water use efficiency from desert to alpine ecosystems in drylands. Agric. For. Meteorol. 298, 108283.
Wu, G., et al., 2015. Elevation-dependent variations of tree growth and intrinsic water-use efficiency in Schrenk spruce (Picea schrenkiana) in the western Tianshan Mountains, China. Front. Plant Sci. 6, 309.
Xu, F., Jia, Y., Peng, H., Niu, C., Liu, J., 2018. Temperature and precipitation trends and their links with elevation in the Hengduan Mountain Region, China. Climate Res. 75 (2), 163–180.
Xu, Q., et al., 2011. Water use patterns of three species in subalpine forest, Southwest China: the deuterium isotope approach. Ecohydrology 4 (2), 236–244.
Yang, M., Gao, X., Wang, S., Zhao, X., 2022. Quantifying the importance of deep root water uptake for apple trees' hydrological and physiological performance in drylands. J. Hydrol. 606, 127471. Amst.
Yang, S., Jong, E.D., 1971. Effect of soil water potential and bulk density on water uptake patterns and resistance to flow of water in wheat plants. Can. J. Soil Sci. 51 (2), 211–220.
Yang, Y., et al., 2019. Sensitivity of potential evapotranspiration to meteorological factors and their elevational gradients in the Qilian Mountains, Northwestern China. J. Hydrol. 568, 147–159.
Zaidi, P., et al., 2007. Importance of secondary traits in improvement of maize (Zea mays L.) for enhancing tolerance to excessive soil moisture stress. Cereal Res. Commun. 35 (3), 1427–1435.
Zapater, M., Bréda, N., Bonal, D., Pardonnet, S., Granier, A., 2013. Differential response to soil drought among co-occurring broad-leaved tree species growing in a 15-to 25-year-old mixed stand. Ann. For. Sci. 70 (1), 31–39.
Zhang, B., et al., 2021. Disentangling the effects of tree and soil properties on the water uptake of a waterlogging tolerant tree in the Yangtze River Delta, China. Forests 12 (11), 1547.
Zhang, B., et al., 2020. Altered water uptake patterns of Populus deltoides in mixed riparian forest stands. Sci. Total Environ. 706, 135956.
Zhang, C., et al., 2017. Differences in water-use strategies along an aridity gradient between two coexisting desert shrubs (Reaumuria soongorica and Nitraria sphaerocarpa): isotopic approaches with physiological evidence. Plant Soil 419 (1), 169–187.
Zheng, Z., Wang, G., 2007. Modeling the dynamic root water uptake and its hydrological impact at the Reserva Jaru site in Amazonia. J. Geophys. Res. Biogeosciences 112 (G4).
Zhou, H., Zhao, W., He, Z., Yan, J., Zhang, G., 2019. Variation in depth of water uptake for Pinus sylvestris var. mongolica along a precipitation gradient in sandy regions. J. Hydrol. 577, 123921. Amst.
Zhou, P., 2013. The Differentiation and Influence Factors of Carbon Sequestration of Typical Vegetation Types in Altitudinal Belts of Gongga Mountain. University of Chinese Academy of Sciences.
Zhu, L., Zhang, H., Gao, X., Qi, Y., Xu, X., 2016. Seasonal patterns in water uptake for Medicago sativa grown along an elevation gradient with shallow groundwater table in Yanchi county of Ningxia, Northwest China. J. Arid Land 8 (6), 921–934.
Zhu, Y., Jia, Z., 2011. Soil water utilization characteristics of Haloxylon ammodendron plantation with different age during summer. Acta Ecol. Sin. 31 (6), 341–346.